AGU PUBLICATIONS

Radio Science

RESEARCH ARTICLE
10.1002/2013RS005270

Key Points:
- A model is proposed for second order statistics of ionospheric scintillation
- The model is validated using a large data set from the last solar maximum period
- A series of equations and approximations for estimating LCR and AFD

Correspondence to:
A. O. Moraes,
alisonaom@iae.cta.br

Citation:
Moraes, A. O., E. R. de Paula, M. T. A. H. Muella, and W. J. Perrella (2014), On the second order statistics for GPS ionospheric scintillation modeling, *Radio Sci.*, *49*, 94–105, doi:10.1002/2013RS005270.

Received 26 JUL 2013
Accepted 2 JAN 2014
Accepted article online 6 JAN 2014
Published online 5 FEB 2014

On the second order statistics for GPS ionospheric scintillation modeling

Alison de Oliveira Moraes[1], Eurico Rodrigues de Paula[2], Marcio Tadeu de Assis Honorato Muella[3], and Waldecir João Perrella[4]

[1]Instituto de Aeronáutica e Espaço/Instituto Tecnológico de Aeronáutica, São José dos Campos, Brazil, [2]Instituto Nacional de Pesquisas Espaciais, São José dos Campos, Brazil, [3]Instituto de Pesquisa e Desenvolvimento, Universidade do Vale do Paraíba, São José dos Campos, Brazil, [4]Instituto Tecnológico de Aeronáutica, São José dos Campos, Brazil

Abstract Equatorial ionospheric scintillation is a phenomenon that occurs frequently, typically during nighttime, affecting radio signals that propagate through the ionosphere. Depending on the temporal and spatial distribution, ionospheric scintillation can represent a problem in the availability and precision for the Global Navigation Satellite System's users. This work is concerned with the statistical evaluation of the amplitude ionospheric scintillation fading events, namely, level crossing rate (LCR) and average fading duration (AFD). Using α-μ model, the LCR and AFD are validated against experimental data obtained in São José dos Campos (23.1°S; 45.8°W; dip latitude 17.3°S), Brazil, a station located near the southern crest of the ionospheric equatorial ionization anomaly. The amplitude scintillation data were collected between December 2001 and January 2002, a period of high solar flux conditions. The obtained results with the proposed model fitted quite well with the experimental data and performed better when compared to the widely used Nakagami-*m* model. Additionally, this work discusses the estimation of α and μ parameters, and the best fading coefficients found in this analysis are related to scintillation severity. Finally, for theoretical situations in which no set of experimental data are available, this work also presents parameterized equations to describe these fading statistics properly.

1. Introduction

Ionosphere causes complications for Global Navigation Satellite Systems (GNSS). Variations on the ionospheric index of refraction cause errors in the estimates of the satellite-receiver pseudoranges and, as consequence, degrade positioning estimation on GNSS-based applications. These errors can be mitigated using models or dual-frequency receivers that are able to estimate the ionospheric delay. In addition to range errors caused by the quiescent ionospheric plasma, the Earth's ionosphere can also affect the performance of GNSS receivers in another way, by the diffraction of radio waves caused by ionospheric plasma density irregularities [*Yeh and Liu*, 1982]. If radio waves propagate through the irregular structures of electron density, phase perturbations are imposed on it and, as the waves propagate toward the receiver on the ground, additional phase variations and also amplitude fluctuations are build up. Amplitude scintillations are consequence of the alternating destructive and constructive interference of different wave fronts arriving simultaneously at the receiver.

Ionospheric scintillations are known to occur more frequently at low and high latitudes [*Aarons*, 1982; *Jiao et al*., 2013]. The most severe cases of amplitude scintillations occur at tropical latitudes, within the belt width of approximately ±15° of magnetic latitude, which corresponds to the region between the northern and southern crests of equatorial ionization anomaly (EIA). The seasonal variation of equatorial scintillations is a function of longitude. For example, in the eastern sector of South America, owing to the large magnetic declination angle (~ −20.0°), a broad maximum of the scintillation activity is observed through the December solstice months [*Sobral et al*., 2002; *Muella et al*., 2013a, 2013b]. The occurrence of ionospheric scintillations also tends to be larger during the period of increased solar activity (close to solar maximum years), when the ionosphere at *F* layer heights is thicker and denser. The low-latitude scintillations generally occur between local sunset and premidnight hours.

The ionospheric scintillation activity at tropical latitudes is strongly controlled by the occurrence of equatorial plasma bubble irregularities. The plasma bubbles are generated by interchange plasma instabilities that

initiate in the bottom side of the equatorial ionospheric *F* region shortly after sunset. As the large-scale plasma bubble structures (of several tens of kilometers in longitudinal width) rise up to great altitudes above the magnetic equator, the magnetic flux tubes associated with the bubbles map their extremities "feet" to off-equatorial latitudes, up to the regions of the EIA crests. Secondary plasma instability processes taking place at the walls of the bubbles can lead to cascading processes that originate a wide spectrum of irregularities with horizontal scale lengths varying from a few kilometers to tens of meters. The strong electron density gradients across the walls and the presence of the smaller scale irregularities may lead to the scatter of the satellite radio signals [*McNamara et al*., 2013]. The maximum contribution to ionospheric amplitude scintillations at GNSS L band frequencies is mainly due to the Fresnel scale size irregularities (~360–400 m).

Ionospheric scintillations can cause sufficient stress to a GNSS receiver that it leads to a loss of receiver lock because of significant reduction in the signal amplitude level. Consequently, this phenomenon can be considered a threat for life critical applications, such as in the civilian air travel [*Seo et al*., 2011]. Thus, the statistical characterization of ionospheric scintillation can yield essential information for the technical and scientific communities involved in the mitigation of errors and failures that cause degradation in the performance of current positioning/navigation applications based on GNSS systems [*Seo et al*., 2009].

Of particular interest is the distribution of signal amplitudes during scintillation events. *Fremouw et al*. [1980] demonstrated that Nakagami-*m* probability density function (pdf) describes well the variability of the amplitude of scintillating signals. However, the statistical tests in the study of Fremouw and co-workers used only 13 time series of L band scintillation to test theoretical pdfs. Furthermore, some of the time series were as short as 20 s. *Hegarty et al*. [2001] developed an amplitude scintillation signal model for Global Positioning System-Wide Area Augmentation System based on a Nakagami-*m* distribution. More recently, *Humphreys et al*. [2009] revisited some of the signal statistics and used a somewhat larger data set to investigate the statistics of scintillating signals. Nevertheless, GPS L1 (1.575 GHz) measurements were limited to 33 time series with lengths varying from 50 to 300 s. *Humphreys et al*. [2009] indicated that either the Nakagami-*m* or the Rice pdf could describe well the distribution of amplitudes that were present in their measurements. The results indicated a slight advantage of the Rice pdf over Nakagami-*m*, but the limited set of measurements would not allow testing the performance of the pdfs for different scintillation levels.

Recently, in the *Moraes et al*. [2012], it has been shown that the ionospheric amplitude scintillation phenomenon can be better modeled by using the α-μ model introduced by *Yacoub* [2007]. This is a more general model that explores the nonlinearity of the propagation medium, associating the physical fading phenomena to the α-μ parameters. *Moraes et al*. [2012] empirically parameterized this distribution as a function of scintillation severity itself, resulting in a more flexible distribution that is specially tailored to the ionospheric scintillation events and that better fits experimental data. The fact of having two parameters that are physically described, instead of just one as in the previous fading models, make this model more flexible, assuring a better agreement with scintillation data. For example, in Moraes et al. (Extended Ionospheric Amplitude Scintillation Model for GPS Receivers, under review to *Radio Science*, 2014), the flexibility of α-μ model is used to estimate the thermal tracking errors in receivers under scintillation.

In the present report, we take advantage of a large set of high-rate measurements of amplitude scintillations, compared to that used in the previous works of *Moraes et al*. [2011, 2012], in order to investigate the temporal characteristics of fading events. Exactly 32 days of nighttime measurements of signal power GPS L1 amplitude data samples (at 50 Hz) have been used in our analysis. These measurements were made by a GPS-based scintillation monitor (named SCINTMON) developed by the Electrical Engineering group from Cornell University, USA [*Beach and Kintner*, 2001]. SCINTMON has a 12-channel correlator that allows the tracking of signals from up to 11 GPS satellites, simultaneously. One channel is dedicated to noise estimation. It was installed in an observatory located at 23.20435°S, 45.86075°W,−17.5° dip latitude, close to the southern crest of the equatorial anomaly and during a period of high solar flux conditions, when typical values of F10.7 were above 150×10^{-22} W/m^2/Hz. The geophysical conditions of the observations allow a broad range of scintillation activity/severity to be investigated. The large data set will provide reliable results about the second order statistics of scintillation, specifically about the temporal fading profile of these events.

In this paper, the α-μ model is validated for second order statistics, namely, level crossing rate (LCR) and average fading duration (AFD). Such a validation is carried out by comparing α-μ formulation against real scintillation data. The AFD and LCR are parameters less used for geophysical studies but highly important for

channel characterization. They are important factors in receiver design especially when diversity combining methods are desired for fading mitigation. They can help to estimate how often the fades will exceed a certain threshold, how long they are expected to last, and how these parameters change according with the scintillation severity. Finally, we determine through empirical fading coefficients the typical LCR and AFD that a GNSS user might expect under similar conditions.

In section 2 we present in detail the α-μ pdf model that will be evaluated in the characterization of the fading statistics. In section 3 we describe the parameters LCR and AFD. Section 4 provides a physical interpretation of α-μ coefficients and its relevance for the validation that will be carried in section 5, where we discuss and present the achieved results in the LCR and AFD validation. Finally, section 6 presents the main concluding remarks.

2. The α-μ Distribution for Scintillation

The S_4 index indicates the severity of amplitude scintillation, and it is defined as the normalized standard deviation of the received signal intensity. It is given by [*Briggs and Parkin*, 1963]

$$S_4 = \sqrt{\frac{\langle I^2 \rangle - \langle I \rangle^2}{\langle I \rangle^2}} \tag{1}$$

where $I = |R|^2$ is the intensity and R is the amplitude envelope of the received power signal. The angular brackets denote time average values.

Moraes et al. [2012] proposed the use of α-μ distribution for amplitude ionospheric scintillation. This model is based on *Yacoub* [2007], and it is a general fading model for which the envelope distribution is parameterized by two coefficients α and μ. This model assumes the signal as a composition of clusters of multipath waves, propagating in a nonhomogeneous environment, where the random phases of the scattered waves have similar delay times with delay-time spreads of different clusters being relatively large. It is assumed to be provoked by an environment in which the scattered radio signals (caused by the regions with random irregular electron density structures) appear in clusters, with the clusters separated from each other by some distance but all affecting the phase of the scattered field in a similar way. The clusters of multipath waves are also assumed to have scattered waves with identical powers. This is indeed a good approximation that leads to a simpler formulation. The resulting envelope is obtained as a nonlinear function of the modulus of the sum of the multipath components, such a nonlinearity manifested in terms of the parameter α [*Yacoub*, 2007]. Meanwhile, the μ parameter is related to the number of multipath components in the propagation environment. Note that the Weibull model makes use of this nonlinear exponent but not of the clustering effect. In the same way, the Nakagami-*m* model makes use of the clustering effect but not of the nonlinear exponent. The alpha-mu model takes both phenomena into consideration.

Variations on the values of α and μ makes α-μ distribution to become special cases like Nakagami-*m*, a Rayleigh, or even a Weibull distribution. For instance, when $\alpha = 2$, α-μ becomes Nakagami-*m* where $m = \mu$, when $\alpha = 2$ and $\mu = 1$ it becomes Rayleigh, or if $\mu = 1$ it turns into a Weibull distribution.

As shown in *Moraes et al.* [2012], for normalized amplitude, the α-μ distribution is given by

$$f_R(r) = \frac{\alpha r^{\alpha\mu-1}}{\xi^{\alpha\mu/2}\Gamma(\mu)} \exp\left(-\frac{r^\alpha}{\xi^{\alpha/2}}\right), \quad \xi = \frac{\Gamma(\mu)}{\Gamma(\mu + 2/\alpha)} \tag{2}$$

where $\Gamma(.) =$ is the Gamma function.

Also, according to *Yacoub* [2007], the α-μ parameters can be estimated based on the equality that involves the moments of α-μ envelope given by

$$\frac{E^2\left(R^\beta\right)}{E\left(R^{2\beta}\right) - E^2\left(R^\beta\right)} = \frac{\Gamma^2(\mu + \beta/\alpha)}{\Gamma(\mu)\Gamma(\mu + 2\beta/\alpha) - \Gamma^2(\mu + \beta/\alpha)}. \tag{3}$$

As suggested in *Yacoub* [2007], the left-hand side of equation (3) can be obtained from field data for arbitrary values of beta. Assuming, for instance, $\beta = 1$ and $\beta = 2$, then two equations with two unknowns, α and μ are set up that can be easily solved. This is the ideal approach for user that has real data available.

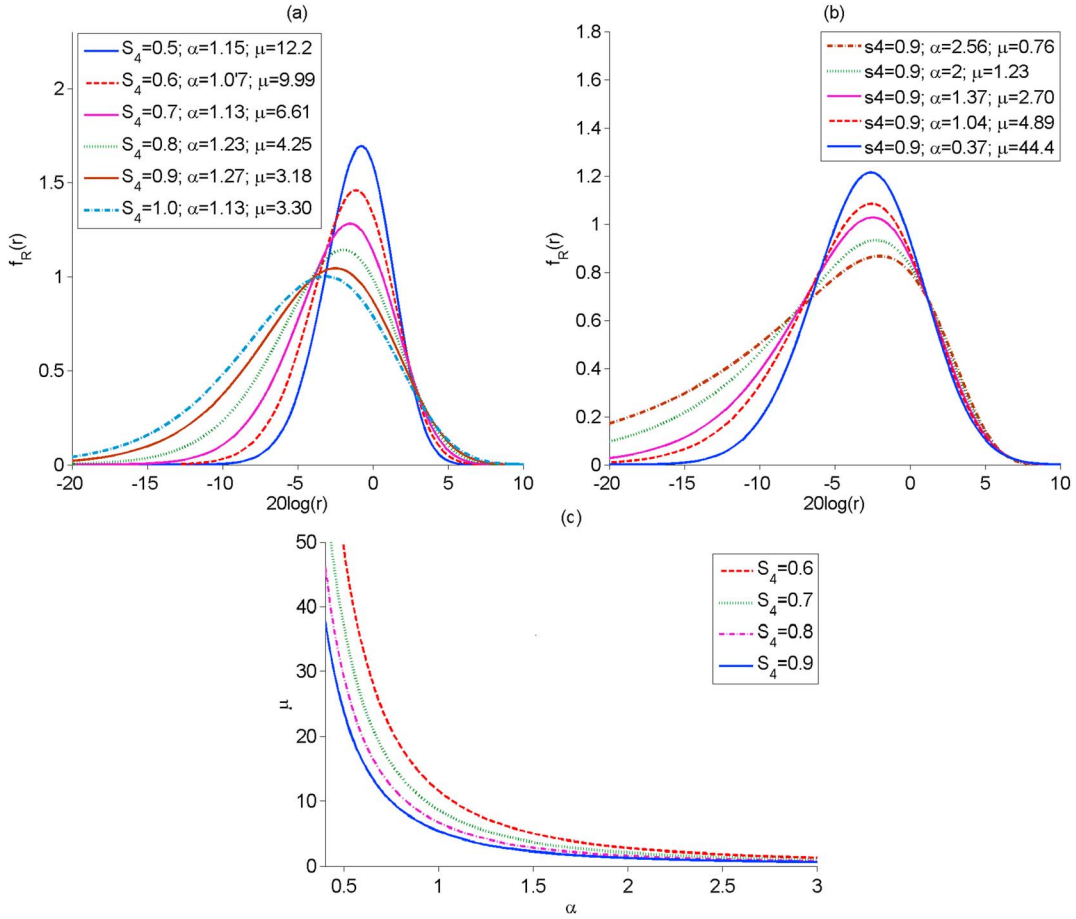

Figure 1. Various shapes of α-μ distribution. (a) The α-μ probability density as a function of scintillation severity based on the parameterization of equation (6) for different values of S_4. (b) Variations on the α-μ probability density for the same scintillation index $S_4 = 0.9$. When $\alpha = 2$ the model becomes the Nakagami-m distribution where $m = \mu$. (c) The α-μ relation where μ decreases as α increases.

Alternatively, for theoretical works or when empirical data is not available, it is possible to establish a relation between m parameter of the Nakagami-m distribution and the α and μ parameters. In this case, assuming $\beta = 2$ in equation (3), we have

$$m = \frac{E^2(R^2)}{\left(E(R^4) - E^2(R^2)\right)}. \tag{4}$$

There will be infinite number of α and μ values that will satisfy the equality of equation (3) for each m of equation (4). Taking $\beta = 2$, and using the relation $m = 1/{S_4}^2$, equation (3) becomes a useful relation between the scintillation index S_4 and the parameters α and μ,

$${S_4}^2 = \frac{\Gamma(\mu)\Gamma(\mu + 4/\alpha) - \Gamma^2(\mu + 2/\alpha)}{\Gamma^2(\mu + 2/\alpha)}. \tag{5}$$

Now the concern is to find the α and μ pairs of parameters that best represents the distribution of amplitude scintillation. Indeed, that is the main benefit of α-μ model; there will be infinite shapes, for the same value of S_4. In *Moraes et al.* [2012], a sequence of tests was conducted to empirically obtain the parameters α and μ for the application of the α-μ model as a function of scintillation index S_4. Based on that, the following approximation that yielded excellent results was proposed,

$$\hat{\alpha} = -17.649\,{S_4}^3 + 39.109\,{S_4}^2 - 27.8218\,S_4 + 7.498 \tag{6}$$

where $\hat{\alpha}$ is the approximate value of α. The corresponding μ can be found by replacing the respective $\hat{\alpha}$ and S_4 in equation (5). Figure 1a illustrates various shapes of the α-μ density function based on equation (6) for $S_4 = 0.5$

up to 1.0. While Figure 1a illustrates α-μ model for different levels of S_4, Figure 1b illustrates five different shapes of α-μ distribution for $S_4 = 0.9$, including $\alpha = 2$ the Nakagami-*m* case where $\mu = m$. In this illustration, the curves vary substantially for the same S_4 value, and therefore, the same value on the equality of moments from equation (3). This flexibility of α-μ model provides a better fit capacity to the scintillation data. It is worth mentioning the inverse relation between α and μ parameters, as α increases μ decreases and vice versa. Figure 1c illustrates α and μ variations for different S_4 values.

3. Level Crossing Rate and Average Fading Duration

The level crossing rate (LCR) is defined as the average value which the envelope *R* crossings a certain level in downward or upward direction, within an observation period. It is defined as [*Yacoub*, 2007]

$$N_R(r) = \int_0^\infty \dot{r} f_{R,\dot{R}}(r, \dot{r}) d\dot{r}, \tag{7}$$

where the upper dot denotes the time derivative of the envelope *R*, and $f_{R,\dot{R}}(r, \dot{r})$ is the joint probability density function of *R* and Ξ.

The average fading duration (AFD) is another parameter derived from the second order statistics. It is defined as the average amount of time that the envelope *R* spends below the specified level. It is represented by [*Yacoub*, 2007]

$$T_R(r) = \frac{F_R(r)}{N_R(r)}, \tag{8}$$

where $F_R(r)$ is α-μ probability distribution function given by *Yacoub* [2007]

$$F_R(r) = \frac{\Gamma(\mu, \mu r^\alpha / \hat{r}^\alpha)}{\Gamma(\mu)}, \tag{9}$$

where $\hat{r}^\alpha = (\Gamma(\mu)/\Gamma(\mu + 2/\alpha))^{\alpha/2}\mu$ according to *Moraes et al*. [2012].

The LCR and AFD for the α-μ distribution are obtained by *Yacoub* [2007] and are given, respectively, by

$$N_R(r) = \frac{\omega \mu^{\mu-0.5} \rho^{\alpha(\mu-0.5)}}{\sqrt{2\pi}\Gamma(\mu) \exp(\mu\rho^\alpha)}, \tag{10}$$

$$T_R(r) = \frac{\sqrt{2\pi}\Gamma(\mu, \mu\rho^\alpha) \exp(\mu\rho^\alpha)}{\omega \mu^{\mu-0.5} \rho^{\alpha(\mu-0.5)}}, \tag{11}$$

where ρ is a scale factor that can be found as

$$\rho = r \sqrt{\frac{\Gamma(\mu + 2/\alpha)}{\Gamma(\mu)}} \mu^{-1/\alpha}. \tag{12}$$

Figures 2 and 3 illustrate these second order statistics for four different levels of scintillation indexes. The α-μ pairs used for these examples are based on the approximation given by equation (6). For comparison purpose, the LCR and AFD are also plotted for $\alpha = 2$, the special Nakagami-*m* case introduced in *Yacoub et al*. [1999].

4. Interpretation of Fading Coefficients

Together with the scintillation index S_4, the intensity or amplitude decorrelation time, τ_0, is another parameter extracted from received signal that helps to characterize the scintillation phenomenon. This parameter is considered a fading rate that is especially used in the study of strong scintillation cases where the S_4 values are not considered a proper indication of the ionospheric perturbations [*Carrano and Groves*, 2010].

According to *Humphreys et al*. [2010], this parameter is also important because the signal tracking is particularly difficult in such cases. A detailed characterization of τ_0 and its likely impacts on the receiver performance can be found in *Carrano and Groves* [2010] and *Moraes et al*. [2011]. In this work, the decorrelation time τ_0 is defined as the time lag at which the autocorrelation coefficients of amplitude falls off by $\exp(-1)$ from its maximum value [*Moraes et al*., 2012].

In this section we exemplify the use of α-μ with the aim of supporting scintillation analysis as an additional tool to describe the fading events. To do that, we examine the influence of α-μ coefficients on the physical

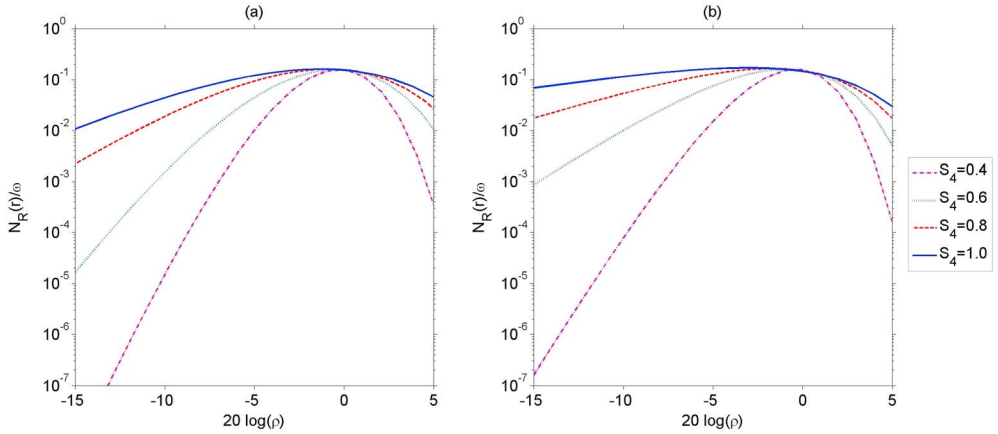

Figure 2. The α-μ level crossing rate as a function of scintillation level. (a) Approximation based on equation (6). (b) Nakagami-*m* case when $\alpha = 2$ and $\mu = \mathrm{m}$.

interpretation of scintillation. First, examining Figure 1b, it is remarkable the differences in the density function for the same S_4 value. It is also possible to note that the larger is the α value, and as consequence, the lower is the μ values, more severe is the scintillation, occupying the lower region of amplitude values with higher probabilities. On Figures 2a and 2b or 3a and 3b it is possible to note that the Nakagami-*m* case ($\alpha = 2$) is more conservative when compared against the α-μ formulation, with the α-μ parameters estimated based on equation (6). In these examples the α values are, respectively, ($\alpha = 1.49$; $\mu = 11.20$), ($\alpha = 1.07$; $\mu = 9.99$), ($\alpha = 1.23$; $\mu = 4.25$), and ($\alpha = 1.13$; $\mu = 3.30$).

As the formulation of equations (10) and (11) are derived from the α-μ probability density, the same behavior will be noted for LCR and AFD. Figure 4 illustrates another example about the relation between the α-μ coefficients and the severity of scintillation. In this case it was chosen two distinct real cases from the data set used in this work, where the S_4 index is close to 0.9 and with the same decorrelation time $\tau_0 = 0.38$ s. Despite both cases presenting the almost the same intensity index and temporal characteristics, their statistics are notably different. Using the equality of moments from equation (3), the α-μ coefficients estimated are, respectively, $\alpha = 2.56$; $\mu = 0.75$ and $\alpha = 0.37$; and $\mu = 46.3$. Analyzing the histograms of Figure 4c, it is possible to note that for a fixed fading index the case with large value of α and small value of μ presents a more spread histogram when compared to the small value of α with large value of μ case. Hence, for the same S_4 index, large values of α and as consequence small values of μ describe worse situations with most likely occurrences of deep fades. Taking the α-μ values estimated by equation (3) for both cases and using them in the formulations given on equations (10) and (11), Figures 4d and 4e illustrate the differences in the LCR and AFD. On these plots it is possible to see

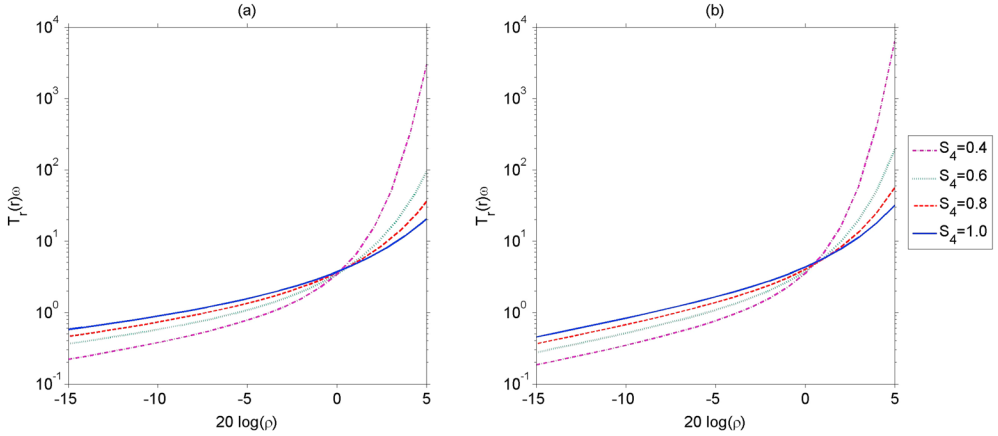

Figure 3. The α-μ average fading duration as a function of scintillation level. (a) Approximation based on equation (5). (b) Nakagami-*m* case when $\alpha = 2$ and $\mu = m$.

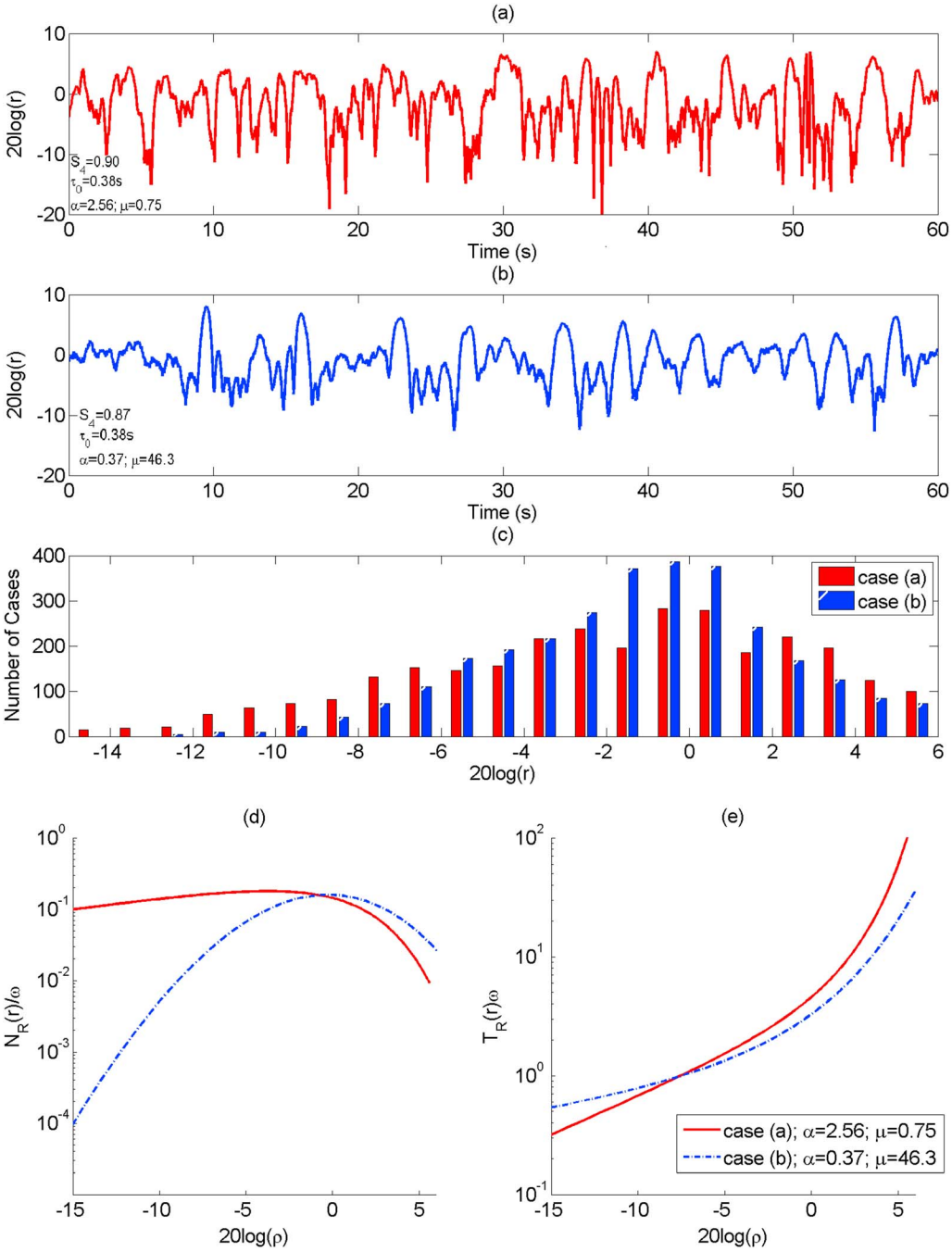

Figure 4. Illustration about influence of fading parameter α. (a and b) Two distinct scintillation cases with approximately same S_4 and temporal characteristics. (c) Histogram highlighting the difference on the statistics of the cases. (d) LCR and (e) AFD for cases in Figures 4a and 4b.

the temporal variation due to the α value. Analyzing Figure 4d, it is implicit that a large value of α represents more crossings for low levels, which means more fades. Observing Figure 4e, it summarizes what is apparent on Figure 4a that is large value of α results in fades that are shorter and more abrupt.

Therefore, for the same value of S_4 index the α value may change significantly and, as a consequence, the severity of scintillation as well. The illustrations and examples presented in this section show that the larger is the value of α, denser will be the tail region on the distribution, which increases the occurrences of deep fades. The temporal consequence of high values of α is an increase in the number of crossings during the fading events together with a decrease in their duration.

Table 1. LCR and AFD Validation Results by Mean Error Deviation as a Function of Scintillation[a]

Test Range 20 Log(r) (dB)		−4.4 up to 3.5	−6.9 up to 4.3	−9.1 up to 5.1	−10.4 up to 5.8	−13 up to 6	−14.8 up to 6	−14.8 up to 6	−13 up to 6
Validation criteria	E[ω]	2.1	2.1	2.2	2.4	2.7	3.1	3.7	3.9
	S_4	**0.3**	**0.4**	**0.5**	**0.6**	**0.7**	**0.8**	**0.9**	**1.0**
Optimun coefficients	α	1.57	1.48	1.68	1.69	1.64	1.82	1.72	1.71
	E[ε_{TR}]	8.04	7.70	7.15	6.42	3.46	7.02	7.60	9.73
	E[ε_{NR}]	7.89	10.08	8.93	6.22	8.02	5.70	7.84	10.33
Moments equality equation (2)	α	1.79	1.71	1.32	1.38	1.53	1.59	1.44	1.35
	E[ε_{TR}]	12.55	10.17	11.58	10.95	4.63	8.92	15.20	17.81
	E[ε_{NR}]	11.82	10.86	19.46	20.61	8.13	11.06	14.63	16.35
Polynomial approximation equation (5)	α	2.19	1.49	1.15	1.07	1.13	1.23	1.27	1.13
	E[ε_{TR}]	22.88	7.73	13.89	16.10	15.37	15.92	18.90	22.33
	E[ε_{NR}]	21.56	10.08	26.68	37.50	30.41	26.77	24.58	27.40
Special Nakagami-m case when $\alpha = 2$	m	11.11	6.25	4.00	2.77	2.04	1.56	1.23	1.00
	E[ε_{TR}]	17.63	18.62	17.69	16.57	13.63	11.88	10.94	13.99
	E[ε_{NR}]	16.40	16.63	15.82	14.87	13.38	15.67	23.05	26.91

[a]The α-μ model with the optimum coefficients presents the best results, in the characterization of second order statistics of scintillation. The equality of moments of equation (3) presents excellent results, especially for $S_4 \leq 0.8$; on the other hand, the Nakagami-m results present good results for $S_4 > 0.8$ cases.

5. Validation Results and Discussion

In this section the second order statistics of α-μ model is tested to evaluate the formulation accuracy of equations (10) and (11) using real scintillation data. The formulations described in the previous sections are compared with results from the processing of a large scintillation data set available to check its performance in the description of these events.

For this study, only data from GPS satellites with elevation greater than 30° were considered. This elevation mask is applied to minimize the use of measurements that could have been affected by nongeophysical sources such as multipath. The measurements of the GPS L1 amplitude were made at INPE's headquarters in São José dos Campos, Brazil (23.20435°S, 45.86075°W, −17.5° dip latitude), a site located near the peak of the equatorial anomaly. We focused our analysis on measurements made between 14 December 2001 and 14 January 2002. This was a period of high solar activity during the previous solar cycle. The strongest amplitude scintillations are known to occur near the equatorial anomaly peak during periods of high solar flux conditions [*Aarons et al*., 1981; *Aarons*, 1982, 1985; *de Paula et al*., 2003; *Whalen*, 2009]. More details about the scintillation database and how data was processed for this validation can be found in the work of *Moraes et al*. [2011] and *Moraes et al*. [2012].

For the LCR and AFD validation, two distinct kinds of tests were performed. In the first sequence of tests, the available data set for each analyzed range of scintillation was treated as a single vector. As an example, all the 243 1 min batches of data corresponding to $S_4 = 0.7$ were grouped, becoming a single vector of amplitude scintillation lasting 243 min. The LCR and AFD rates were computed from this vector, excluding only the fades and crossings artificially introduced by joining together the individual 1 min batches. These rates were compared with the predictions by the theoretical formulations of equations (10) and (11).

In the second approach the empirical LCR and AFD were computed, and the estimation results compared with the corresponding ones form the theoretical formulation of equations (10) and (11) for every single minute. In both approaches, the envelope R was filtered by a eighth-order Butterworth low-pass filter with cutoff frequency of 4 Hz. Tables 1 and 2 present, respectively, the results from these approaches as a function of S_4. The adopted error criteria was the mean absolute error deviation, defined as [*Dias and Yacoub*, 2009]

$$\varepsilon = \frac{1}{N}\sum_{i=1}^{N}\frac{|y_i - x_i|}{x_i}. \tag{13}$$

In Table 1, it is presented the results of α-μ model for four different possibilities. First, it was found that the α-μ pair that minimizes the mean error deviation for each level of scintillation tested presented here as optimum coefficients. Then the equality of moments from equation (3) was used to estimate the α-μ coefficients.

Table 2. LCR and AFD Validation Results for the Minute to Minute Tests[a]

Test Range 20 Log(r) (dB)		±2	±2.5	±3	±3	±4.5	±5.2	±6	±7
Validation criteria	E[ω]	2.0	2.1	2.2	2.4	2.6	3.0	3.4	3.7
	S_4	**0.3**	**0.4**	**0.5**	**0.6**	**0.7**	**0.8**	**0.9**	**1.0**
Optimun coefficients	α	1.57	1.48	1.68	1.69	1.64	1.82	1.72	1.71
	E[ε_{TR}]	23.08	17.81	16.33	14.67	13.72	13.16	11.37	12.23
	E[ε_{NR}]	16.23	13.58	12.40	11.02	9.82	9.61	8.07	7.63
Moments equality equation (2)	E[α]	1.79	1.71	1.32	1.38	1.59	1.53	1.44	1.35
	E[ε_{TR}]	30.73	26.22	20.95	19.55	20.81	17.64	15.43	17.60
	E[ε_{NR}]	17.72	16.35	14.41	14.87	15.15	13.71	13.07	14.38
Polynomial approximation equation (5)	α	2.19	1.49	1.15	1.07	1.13	1.23	1.27	1.13
	E[ε_{TR}]	26.40	17.86	14.17	13.18	13.22	12.46	12.27	14.19
	E[ε_{NR}]	18.48	13.58	11.39	10.66	10.63	10.34	10.77	12.03
Special Nakagami-m case when $\alpha = 2$	m	11.11	6.25	4.00	2.77	2.04	1.56	1.23	1.00
	E[ε_{TR}]	24.72	21.23	17.95	16.57	15.75	14.43	12.40	13.73
	E[ε_{NR}]	17.70	15.69	13.81	12.44	11.26	10.63	8.26	8.49

[a]The α-μ optimum pairs for the tests performed on Table 1 together with the approximation of equation (6) reached the best results in these tests. The Nakagami-m model presented quite reasonable results especially for higher levels, while the equality of moments has performed coarsely.

Additionally, the approximation of equation (6) to parameterize the α-μ pairs as a function of S_4 for the pdf is also tested. Finally, the special Nakagami-m case introduced in the work of *Yacoub et al.* [1999] is also evaluated.

The α-μ pairs that achieved the optimum results on Table 1 are used in the minute to minute tests. The equality of moments from equation (3) is used for every minute to estimate the α-μ pairs. The polynomial approximation and the Nakagami-m case were also tested. For the minute to minute validation, the range of values of R is reduced if compared with the values of Table 1 owing to the limited number of samples available to conduct the test. Table 2 presents the average mean error deviation for theses tests.

From Table 1, it is seen that the optimum results show a very good agreement with field data for both AFD and LCR, which can be seen in Figures 5 and 6. The results for equality of moments are also fairly accurate, especially for higher levels of scintillation. The Nakagami-m results might be considered as a rough estimation, while the polynomial approximation is the one with the worst results.

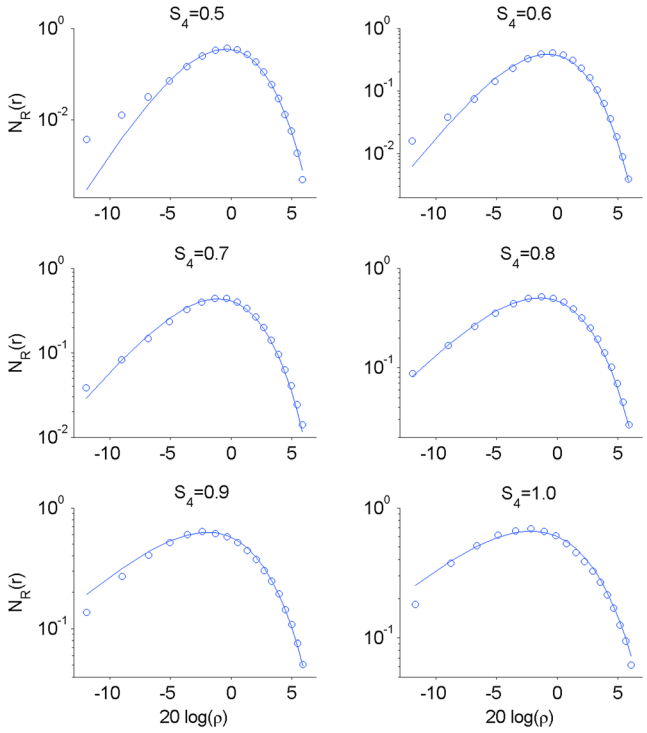

Figure 5. Empirical LCR (crossings/second) versus theoretical α-μ model.

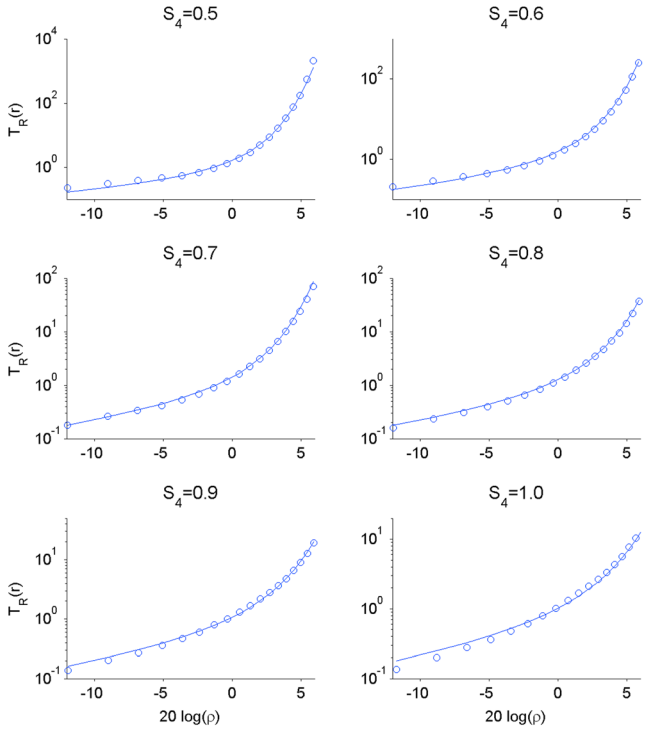

Figure 6. Empirical AFD (seconds) versus theoretical α-μ model.

For the minute to minute tests, the α-μ pairs that minimized the ε_{TR} and ε_{NR} (optimum coefficients) in the first sequence reached some of the best results together with the approximation of equation (6). The Nakagami-*m* results in these cases presented quite reasonable results especially for higher levels of scintillation. Unlike the previous result, for these cases the equality of moments has performed coarsely. It is important to note that this approach had limited range of *R* because of the observation period of 1 min.

Comparing the theoretical formulation of LCR and AFD against scintillation data, it is possible to conclude that for mid and low levels of scintillation these models underestimate the lower values of *R*, which is the deeper region of the fades. Analyzing Figures 5 and 6, it is possible to note that for $S_4 < 0.7$ the fading duration and the number of crossings is bigger than the predicted by the models. On the other hand, for $S_4 > 0.7$ these models tend to become more conservative, predicting longer fades and more crossings for the deeper region.

As shown in Tables 1 and 2, the performance of the α-μ model is better than that of the Nakagami-*m* one. Figure 7 shows two examples that illustrate such differences. The left plot is one example of mid level of

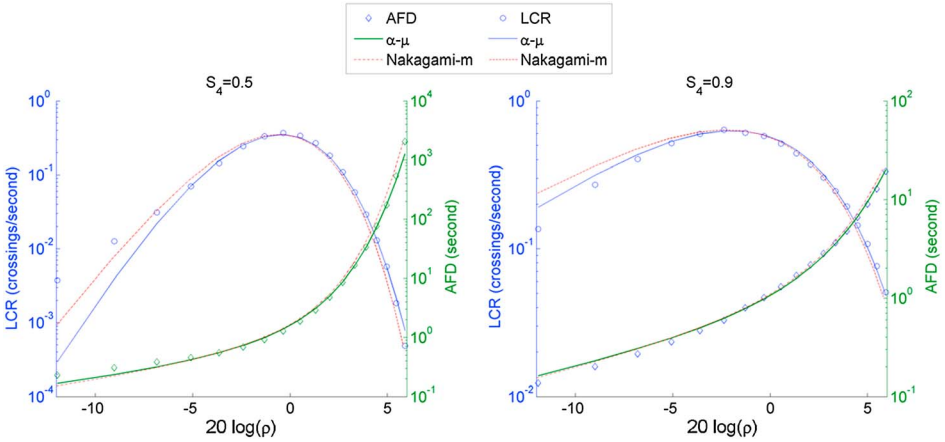

Figure 7. Two examples of LCR and AFD comparing the empirical results versus theoretical formulation of α-μ and Nakagami-*m* models.

scintillation, where both the formulations are underestimated in the fading region but the Nakagami-*m* being more realistic in the number of crossings for lower values of *R*. However, for the remaining range of *R* the α-μ estimation is more accurate. In this example, the AFD of Nakagami-*m* estimation is rough for all the ranges tested, while α-μ keeps on track for most of the values.

In the right plot of Figure 7 is presented an example of high level of scintillation. Again, the α-μ model presents a much better fit, especially for LCR where the Nakagami-*m* presents a more conservative and less realistic estimation. For AFD, the α-μ result is better, fitting very well for $R > 1$, but failing on the estimation for lower values of *R*. In this case Nakagami-*m* is less accurate too.

6. Summary and Conclusions

In this paper, the α-μ model was proposed and validated for second order statistics of scintillation. The validation was carried out by comparing level crossing rate (LCR) and average fading duration (AFD) formulations against real scintillation data. Additionally, the Nakagami-*m* model which is widely used in for first order statistics of scintillation is also tested and validated for second order.

Before the validation process, a discussion on the influence of the α-μ parameters and how they can be used to support scintillation analyses was carried out. The relation between α-μ parameters and scintillation severity was highlighted through examples.

The validation results showed that the α-μ model is the one that best characterizes second order statistics of amplitude scintillation of those considered here. For the LCR and AFD, the α-μ formulation presented excellent results when compared with field data. The only exception was for high levels of scintillation and low values of *R* where this model presents to be a little bit conservative but still much more realistic than the Nakagami-*m* model. For the LCR and AFD a polynomial approximation that parameterizes the α-μ pairs as a function of S_4 index was tested. For analyses involving low ranges of *R* and short data this approximation presented good results, but for extended investigation it only gives a rough estimate.

The validation carried out in this work allows GNSS users to relate their measurements with statistical models and as consequence with the dynamics of the process through the time. Therefore, the formulation presented in this paper allows users to estimate the number of crossings and the average duration that the envelope *R* remains under a particular level. This may be used to estimate outage rate and duration, and as consequence the conditions for which the receiver may loose lock during events of ionospheric scintillation.

Moreover, the fading coefficients presented in this work determine the typical LCR and AFD values for scintillation environment at low latitude under similar zonal drift conditions. These values might help to estimate rates that express how vulnerable a user might be due to deep fades occurrences. Besides that, those coefficients may help on the design of more robust receivers, less susceptible to ionospheric conditions, especially for critical applications like defense systems, high dynamics sensors for navigation, and augmentation systems like SBAS and GBAS.

It is important to note that the validation of α-μ model and the fading coefficients presented in this work are strictly related to GPS L1 users under solar maximum conditions. The flexibility of the model, the use of the equality of moments from equation (3), and the validation results suggest the feasibility of the model that may be considered to other solar cycle periods as well for other GNSS users.

Additionally, this validation creates the possibility of using the LCR and AFD for scintillation analyses, which might help to understand physical mechanisms of scintillation. For example, possible future work relating the α-μ parameters might be used to provide us relevant information about the spatial variations of the electron density through the medium and the drift velocities of scintillation-producing irregularities perpendicular to the raypath from the orbiting satellites.

Acknowledgments
The authors are grateful to Fabiano Rodrigues from University of Texas at Dallas and Emanoel Costa from Centro de Estudos em Telecomunicações da Pontifícia Universidade Católica do Rio de Janeiro (CETUC/PUC-Rio) for numerous discussions and suggestions regarding the use of α-μ model. AOM wishes to thank the Instituto de Aeronáutica e Espaço (IAE), where he works as a research engineer, for supporting and assisting his cooperation with INPE and ITA. MTAHM would like to thank the support from CNPq under process 308017/2011-0. ERP is grateful for the partial support from AFOSR FA9550-10-1-0564 and CNPq 305684/2010-8 grants.

References

Aarons, J. (1982), Global morphology of ionospheric scintillations, *Proc. IEEE*, *70*(4), 360–378.
Aarons, J. (1985), Construction of a model of equatorial scintillation intensity, *Radio Sci.*, *20*(3), 397–402, doi:10.1029/RS020i003p00397.
Aarons, J., J. P. Mullen, H. E. Whitney, E. M. MacKenzie, and S. Basu (1981), S Microwave equatorial scintillation during solar maximum, *Radio Sci.*, *16*, 939–945.
Beach, T. L., and P. M. Kintner (2001), Development and use of a GPS ionospheric scintillation monitor, *IEEE Trans. Geosci. Remote Sens.*, *39*, 918–928, doi:10.1109/36.921409.

Briggs, B. H., and I. A. Parkin (1963), On the variation of radio star and satellite scintillations with zenith angle, *J. Atmos. Terr. Phys.*, *25*, 339–366, doi:10.1016/0021-9169(63)90150-8.

Carrano, C. S., and K. M. Groves (2010), Temporal decorrelation of GPS satellite signals due to multiple scattering from ionospheric irregularities. Proc. of the 2010 Institute of Navigation ION GNSS meeting.

De Paula, E. R., F. S. Rodrigues, K. N. Iyer, I. J. Kantor, M. A. Abdu, P. M. Kintner, B. M. Ledvina, and H. Kil (2003), Equatorial anomaly effects on GPS scintillations in Brazil, *Adv. Space Res.*, *31*(3), 749–754.

Dias, U. S., and M. D. Yacoub (2009), On the α-μ autocorrelation and power spectrum functions: Field trials and validation, in *IEEE Global Communications Conference (GLOBECOM'09)*, pp. 1–6, IEEE, Honolulu, USA, 30 Nov.- 4 Dec., doi:10.1109/GLOCOM.2009.5425619.

Fremouw, E. J., R. C. Livingston, and D. A. Miller (1980), On the statistics of scintillating signals, *J. Atmos. Terr. Phys.*, *42*, 717–731.

Hegarty, C., M. B. El-Arini, T. Kim, and S. Ericson (2001), Scintillation modeling for GPS-Wide Area Augmentation System receivers, *Radio Sci.*, *36*, 1221–1231.

Humphreys, T. E., M. L. Psiaki, J. C. Hinks, and P. M. Kintner Jr. (2009), Simulating ionosphere-induced scintillation for testing GPS Receiver Phase Tracking Loops, *IEEE J. Sel. Top. Sign. Proces.*, *3*, 707–715, doi:10.1109/JSTSP.2009.2024130.

Humphreys, T. E., M. L. Psiaki, and P. M. Kintner Jr. (2010), Modeling the effects of ionospheric scintillation on GPS carrier phase tracking, *IEEE Trans. Aerosp. Electron. Syst.*, *46*, 1624–1637.

Jiao, Y., Y. T. MOrton, S. Taylor, and W. Pelgum (2013), Characterization of high-latitude ionospheric scintillation of GPS signals, *Radio Sci*, *48*, doi:10.1002/2013RS005259.

McNamara, L. F., R. G. Caton, R. T. Parris, T. R. Pedersen, D. C. Thompson, K. C. Wiens, and K. M. Groves (2013), Signatures of equatorial plasma bubbles in VHFsatellite scintillations and equatorial ionograms, *Radio Sci.*, *48*, 89–101, doi:10.1002/rds.20025.

Moraes, A. O., F. S. Rodrigues, W. J. Perrella, and E. R. de Paula (2011), Analysis of the characteristics of low-latitude GPS amplitude scintillation measured during solar maximum conditions and implications for receiver performance, *Surv. Geophys.*, *33*(5), 1107–1131, doi:10.1007/s10712-011-9161-z.

Moraes, A. O., E. R. de Paula, W. J. Perrella, and F. S. Rodrigues (2012), On the distribution of GPS signal amplitudes during the low-latitude ionospheric scintillation, *GPS Solutions*, doi:10.1007/s10291-012-0295-3.

Muella, M. T. A. H., E. R. de Paula, and A. A. Monteiro (2013a), Ionospheric scintillation and dynamics of Fresnel-scale irregularities in the inner region of the equatorial ionization anomaly, *Surv. Geophys.*, *34*, 233–251, doi:10.1007/s10712-012-9212-0.

Muella, M. T. A. H., E. R. de Paula, and O. F. Jonah (2013b), GPS L1-frequency observations of equatorial scintillations and irregularity zonal velocities, *Surv. Geophys.*, doi:10.1007/s10712-013-9252-0.

Seo, J., T. Walter, T. Y. Chiou, and P. Enge (2009), Characteristics of deep GPS signal fading due to ionospheric scintillation for aviation receiver design, *Radio Sci.*, *44*, RS0A16, doi:10.1029/2008RS004077.

Seo, J., T. Walter, and P. Enge (2011), Availability impact on GPS aviation due to strong ionospheric scintillation, *IEEE Trans. Aerosp. Electron. Syst.*, *47*(3), 1963–1973, doi:10.1109/TAES.2011.5937276.

Sobral, J. H. A., M. A. Abdu, H. Takahashi, M. J. Taylor, E. R. de Paula, C. J. Zamlutti, M. G. Aquino, and G. L. Borba (2002), Ionospheric plasma bubble climatology over Brazil based on 22 years (1977–1998) of 630 nm airglow observations, *J. Atmos. Sol. Terr. Phys.*, *64*(12–14), 1517–1524, doi:10.1016/S1364-6826(02)00089-5.

Whalen, J. A. (2009), The linear dependence of GHz scintillation on electron density observed in the equatorial anomaly, *Ann. Geophys.*, *27*, 1755–1761.

Yacoub, M. D. (2007), The α-μ distribution: A physical fading model for the stacy distribution, *IEEE Trans. Veh. Technol.*, *56*, 27–24, doi:10.1109/TVT.2006.883753.

Yacoub, M. D., J. E. V. Bautista, and L. G. R. Guedes (1999), On higher order statistics of the Nakagami-m distribution, *IEEE Trans. Veh. Technol.*, *V48*(3), 790–794.

Yeh, K. C., and C. H. Liu (1982), Radio wave scintillations in the ionosphere, *Proc. IEEE*, *70*(4), 324–360, doi:10.1109/PROC.1982.12313.